Ultrastructural Characteristics of Carcinogen-Induced Nondysplastic Changes in Tracheal Epithelium

A. J. P. Klein-Szanto, MD, D. C. Topping, PhD, C. A. Heckman, PhD, and Paul Nettesheim, MD

Nondysplastic hypotrophic and metaplastic epithelial alterations induced by dimethylbenz(*a*)anthracene in isogenic tracheal transplants were studied by light and electron microscopy 3-24 months after cessation of a 4-week carcinogen exposure. Hypotrophic epithelium observed at all time points was characterized by the presence of nonciliated cells that adopted either cuboidal or squamous shapes, forming simple or bistratified epithelia. Most of these cells, as well as some metaplastic cells, exhibited features of mucin-secreting cells. The metaplastic epithelia showed nonkeratinizing squamous metaplasia, closely related to transitional metaplasia, and keratinizing squamous metaplasia, which presented either an atrophic or an acanthotic epithelium. Although many of these epithelia showed morphologic features of normal stratified epithelia, several nonkeratinizing squamous metaplasias and acanthotic keratinizing squamous metaplasias exhibited some irregularities, probably representing very early atypical ultrastructural features (ie, perinuclear concentration of tonofilament bundles, the presence of dark and clear basal epithelial cells, interruptions and alterations of the basal lamina). These features were not observed in a group of early squamous metaplasias studied for comparative purposes 2 weeks after cessation of dimethylbenz(*a*)anthracene exposure, which were characterized by a combination of degenerative phenomena and increased cell proliferation. (Am J Pathol 98:61-82, 1980)

VARIOUS EPITHELIAL CHANGES are known to occur in the respiratory tract of humans and animals exposed to carcinogenic agents.[1-3] To what extent these lesions are morphologic manifestations of the underlying carcinogenesis process is controversial, even though various plausible schemes have been presented describing a sequence of morphologic events presumed to characterize the multiphasic evolution of cancer.[2,4,5] Several major obstacles have frustrated attempts to elucidate the morphogenesis of neoplasia in respiratory tract tissues. Some of these are inherent in the study of carcinogenesis, such as the acute and chronic cytotoxicity of carcinogens; others are related to the anatomic and physiologic complexities of the respiratory tract system.[6]

To alleviate some of these problems, we have developed a simplified model for respiratory carcinogenesis studies in which only one segment of

From the Biology Division, Oak Ridge National Laboratory, Oak Ridge, Tennessee.

Supported by the National Cancer Institute, the National Institute of Environmental Health Sciences under Interagency Agreement 40-662-77, and the Office of Health and Environmental Research, US Department of Energy, under contract W-7405-eng-26 with the Union Carbide Corporation.

Accepted for publication July 23, 1979.

Address reprint requests to Dr. A. J. P. Klein-Szanto, Oak Ridge National Laboratory, P.O. Box Y, Oak Ridge, TN 37830.

0002-9440/80/0109-061$01.00

the respiratory tract, namely, the trachea, is exposed to known quantities of carcinogen for a limited period of time.[6] We are therefore able to study epithelial lesions arising with time as a result of a well-quantified carcinogenic insult in a defined area of respiratory tract epithelium.

The present report describes the first ultrastructural study of epithelial changes in tracheal transplants (TTs) and forms part of a series of communications in which the new possibilities offered by the tracheal transplant model are exploited in studies of the morphogenesis of respiratory tract carcinogenesis.[7-10] In all our studies related to this topic, an exposure-free interval was interposed between the carcinogenic insult and the beginning of the main part of the morphologic studies. This was done to allow the acute cytotoxic changes, which confound so many morphogenesis studies in humans and animals, to subside.

In this and the accompanying report,[7] we are attempting to define the major epithelial changes occurring as a result of carcinogen exposure at the histochemical and ultrastructural level. Subsequent reports will deal with morphometric and autoradiographic analysis of carcinogen-induced lesions, as well as the dynamics of the appearance and disappearance of various epithelial alterations and the emergence of neoplastic lesions.[8-10] The present report defines the nondysplastic changes ultrastructurally; the accompanying paper deals with the dysplastic and early neoplastic lesions.

Materials and Methods

Animals

Ten-week-old inbred Fischer 344 female rats, bred and maintained in a barrier facility, were used. They were free of the common respiratory pathogens of rats, including mycoplasmas.

Tracheal Transplants

The donor tracheas were surgically exposed and flushed with Hanks' balanced salt solution, then attached at either end to a 3.0-cm length of sterile polyethylene tubing with silk sutures to prevent curling of the transplant.

The skin of isogenic recipient rats was prepared by clipping, chemical depilation, and sterilization with 2% peracetic acid. A 2.0-cm incision was made on the dorsal midline between the shoulders, and subcutaneous pockets were prepared on either side by blunt dissection. A donor trachea was inserted in each pocket, and the wound was closed with metal clips. Thus, each recipient carried two transplants.

Twenty-eight days after transplantation, a carcinogen pellet was inserted into the lumens through the cut end of each transplant, which was then ligated with a silk suture.

Carcinogen Pellets

Dimethylbenz(*a*)anthracene (DMBA) powder (Eastman Kodak Co., Rochester, NY) was melted at 122 C and mixed with melted laboratory-grade white beeswax. The mixture was

formed in a pellet-maker into cylindrical pellets 1.6 mm in diameter and 15 mm long, with a volume of approximately 30 μl and a weight of 24.45 ± 1.1 mg. The concentrations of DMBA were adjusted on a weight basis. Control pellets consisted of beeswax without carcinogen.

Experimental Procedures

Six groups of 4–8 TTs were exposed to pellets containing either 165 or 200 μg DMBA for 4 weeks. Control transplants were exposed to beeswax pellets without the carcinogen and studied at 65 weeks. Groups of transplants from both dose levels were harvested at 2, 12, 16, 24, 48, and 96 weeks after the cessation of carcinogen exposure. The animals were anesthetized with methoxyflurane, their abdomens were opened, and the portal veins were severed. The subcutaneous TTs were dissected and flushed with 3% glutaraldehyde in *s*-collidine buffer. The tracheas were transversely cut in 1–2-mm rings and fixed for 2 hours in the same chilled fixative. After they were washed in 0.05 M cacodylate buffer, the tissues were postfixed in 2% osmic acid in 0.1 M cocodylate buffer. A total of 528 blocks were dehydrated in graded acetone solutions and embedded in Epon 812.

Light Microscopy

Semithin sections 1 μ thick were stained with toluidine blue, and areas appropriate for electron microscopy were selected by light microscopy. The following tracheas were selected for further histochemical and electron-microscopic studies: 10 tracheas containing selected areas of hypotrophic epithelium and 20 tracheas containing selected areas of squamous metaplasias (4 containing 2-week-old alterations and the rest representing the later changes). The relative percentage of surface area covered by the altered epithelia was determined by counting, with the aid of an ocular grid, the number of fields showing the studied alterations in the tracheal circumference.[11] The periodic acid–Schiff (PAS) reaction alone, both with and without previous amylase digestion, and PAS followed by alcian blue (AB) staining at either pH 2.6 or 1 were carried out in 1-μ–thick Epon sections.[12] As the AB staining of epithelial mucosubstances proved to be almost negative in the plastic-embedded material, an additional 15 paraffin blocks, derived from three groups of five different TTs treated with 200 μg of DMBA for 2, 4, and 20 weeks, respectively, were studied with the same histochemical techniques.

Electron Microscopy

Ultrathin sections from the selected blocks containing hypotrophic and metaplastic epithelia were cut and double-stained with uranyl acetate and lead citrate. A Hitachi HU-11 and a Siemens 101 electron microscope were used during these studies.

Results

The main objective of this study was to describe the ultrastructural characteristics of the nondysplastic epithelial changes present in tracheas many months after exposure to DMBA. The dysplastic lesions found in the same tracheas will be discussed in the accompanying paper. We have for the most part excluded epithelial changes occurring during or shortly after carcinogen exposure, ie, acute toxic changes. Most of the tissues were sampled between 3 and 24 months after the termination of exposure.

The major nondysplastic changes observed were the following: a) Hypotrophic mucociliary epithelium was found mostly in control tracheas

(covering approximately 50% of the surface); this had all the essential ultrastructural features of normal tracheal epithelium and was the typical lining of TTs 12 to 18 months old. b) Hypotrophic nonciliated epithelium was found in control (~50% of the surface area) and DMBA-exposed tracheas (50–90% of the surface area). c) Various types of squamous metaplasias were found exclusively in carcinogen-exposed tracheas (5–10% of the surface area). Since the morphologic characteristics of these three main types of epithelial alterations were stable throughout the 24-month study, each category can be discussed without regard to the time at which the tissue samples were actually obtained. The mucociliary epithelium commonly found in control tracheas and also seen, though much less commonly, in DMBA-exposed tracheas had maintained all typical characteristics of tracheal epithelium, except for partial loss and abnormal morphologic features of cilia. Cells containing neutral glycoproteins were common. Acid mucosubstances were detected with PAS–AB stain at pH 2.6, and to a lesser extent at pH 1.

Two types of hypotrophic epithelia commonly seen in DMBA-exposed tracheas are illustrated in Figures 1 and 2. Amylase-resistant PAS-positive granules were commonly found in this epithelium (Figure 1) as well as some material positive for AB (pH 2.6). At the ultrastructural level, the morphologic features of the cuboidal and flat, poorly differentiated cells were similar (Figure 3). The cells were rich in mitochondria, ribosomes, and rough endoplasmic reticulum and also contained an active Golgi apparatus and numerous intracytoplasmic filaments. Secretory vesicles were commonly seen; the surface showed short microvilli. Most of these cells clearly had the characteristics of mucus-secreting cells. However, some of the extremely flattened cells were almost devoid of cytoplasmic organelles. Ciliated cells were absent in this type of epithelium, indicating that a severe defect in differentiation and the function of the epithelium existed.

The metaplastic epithelia were essentially of two types, nonkeratinizing stratified squamous epithelium and orthokeratinizing stratified squamous epithelium. Lesions in which both types of metaplasia occurred in juxtaposition were common. Parakeratinization was occasionally observed in the thicker metaplasias. The nonkeratinizing lesions consisted of a relatively thick epithelium in which the often nucleated superficial layer (Figure 4) exhibited large numbers of loosely disposed cytoplasmic filaments, few filament bundles, an absence of interfilamentous dense matrix, and cytoplasmic organelles such as ribosomes and endoplasmic reticulum (Figures 6 and 7). In several cases the superficial cells were not flat but rather voluminous, ovoid or polyhedral in shape, and straddled several cells of

the underlying stratum (Figure 6). This type of superficial disposition in a stratified epithelium is equivalent to the so-called transitional metaplasia. The keratinizing metaplastic epithelia occurred in an atrophic variety (5 cell layers) and in an acanthotic variety (10 cell layers). Both were characterized by a superficial orthokeratinized horny layer and the presence of a variably prominent granular layer (Figures 5, 8, and 9).

The basal and spinous cells of all types of squamous metaplasia usually had characteristics reminiscent of those found in normal stratified squamous epithelium (Figure 9), such as esophageal epithelium. Some atypical features were occasionally found, especially in the acanthotic and the nonkeratinizing lesions. These abnormal features were observed mainly in the basal layer, where two types of basal epithelial cells coexisted. One of these types (dark cell) exhibited a general electron-dense appearance due to an increased density of cytoplasmic filament-bundles and organelles and a denser nuclear chromatin pattern (Figure 10). The other cell type (clear cell), more ovoid and larger than the dark cell, showed a relatively electron-lucent cytoplasm with a decreased density of organelles and filament bundles and a looser chromatin pattern (Figure 11). The basal lamina showed frequent interruptions and duplications of the lamina densa, and in many cases it was totally absent (Figure 12). In the spinous and superficial layers the abnormal features included cells with both keratinocyte and secretory cell features (Figure 7), cells with intercellular or intracellular cyst-like formations, and cells with increased amounts of tonofilaments (sometimes marginated on the periphery of the cell and sometimes perinuclearly centralized) (Figure 13).

We compared these late metaplasias with those appearing early during the first 2 weeks of carcinogen exposure. Many similarities existed. Nonkeratinizing squamous metaplasias were predominant among these early toxic changes. Amylase-resistant PAS-positive material was frequently observed in the spinous layer of both metaplasias, but only the early metaplasias commonly showed AB staining of the superficial layers at pH 2.6 (Figure 14), and much less at pH 1.

The early metaplasias were also characterized by the presence of large numbers of intraepithelial inflammatory cells (Figure 15) and by degenerative changes such as endoplasmic reticulum dilation, mitochondrial swelling, large numbers of autophagosomes, and other lysosomal structures indicative of a toxic reaction.

Discussion

As much as 90% of the epithelium in DMBA-exposed tracheas and up to 50% of the epithelium in control tracheas was of the poorly differentiated,

nonciliated type, and showed histochemical and ultrastructural evidence of mucus production. The loss of ciliated cells and the establishment of a hypotrophic and more "primitive" epithelial lining has also been described by others [13-18] and appears to be a sign of nonspecific residual damage and a chronic defect in cell differentiation. Squamous metaplasia was observed only in carcinogen-exposed tracheas.

All the late metaplasias were defined as differentiated, orderly epithelia without atypias by light-microscopic criteria. Although in a few instances irregularities could be seen at the light-microscopic level, our study revealed ultrastructural characteristics that previous publications have often associated with preneoplastic and neoplastic alterations. In the late nonkeratinizing and acanthotic metaplasias we observed the following atypical features: high tonofilament concentration in the endoplasm, interruptions of basal lamina, and the appearance of dark and clear basal epithelial cells. The dark and clear basal cells, although described in the normal epidermis,[19] have been found in increased numbers in carcinogen- and/or promoter-treated epidermis.[20,21] The absence or interruption of the lamina densa and the formation of cytoplasmic projections in the area of epithelium–connective-tissue interface, found in several diseased epithelia, has also been observed by other investigators.[22-24] Kilburn and McKenzie observed these changes in the airways of hamsters shortly after exposure to aldehydes.[25] Its significance in carcinogenesis is unclear. Conceivably such areas might be "points of least resistance" for cells capable of invasion.

Trump et al [5] and Becci et al [18] concluded, on the basis of detailed histochemical and ultrastructural studies of human and hamster airways, that metaplastic and neoplastic cells were derived from the mucous cells of the respiratory epithelium. Confirming these authors' observations, we noted the presence of neutral and acid mucosubstances in the hypotrophic and most of the metaplastic epithelia. Although acid mucosubstances were detected with the PAS–AB stain at both pH 2.6 and 1, the contribution of sulfated mucosubstances was small, as revealed by weak positive staining at pH 1. Evidence of mucin secretion did not always include outright formation of secretory material but indirect features characteristic of synthetic activity, such as enlarged nucleoli, prominent Golgi complexes, and increased rough endoplasmic reticulum.

A comparison was made between early and late squamous metaplasias. While the two alterations were similar in many respects, there were also a number of differences. The early metaplasias were characterized by a combination of degenerative alterations, similar to those described by Barrett et al [26] in ischemic tracheal explants, and increased cell prolifera-

tion, with an increment in the synthetic activities of mucin and/or cytoplasmic filaments. In contrast to the diffuse distribution of these metaplasias, the late squamous metaplasias presented a patchy distribution that arose long after the carcinogen had been removed from the TTs, and did not present major involutional changes.

Our studies on the fate of late squamous metaplasias without (or with only very mild) cellular atypia suggest that many of them eventually regress and others remain stationary, with no indication of progression to more advanced lesions.[9,10] Whether such metaplastic lesions harbor initiated or partially transformed cells that might be propelled to more advanced stages if exposed to a suitable promoting agent remains an interesting speculation.

References

1. Shabad LM, Pylev LN: Morphological lesions in rat lungs induced by polycyclic hydrocarbons, Morphology of Experimental Respiratory Carcinogenesis. Edited by P Nettesheim, MG Hanna Jr, JW Deatherage Jr. Oak Ridge, Tenn, US Atomic Energy Commission, 1970, pp 227–242
2. Stenbäck F: Morphologic characteristics of experimentally induced lung tumors and their precursors in hamsters. Acta Cytol 17:476–486, 1973
3. Nettesheim P, Schreiber H: Advances in experimental lung cancer research. Handbuch Allg Pathol vi/7:603–691, 1975
4. Melamed MR, Zaman MB, Flehinger BJ, Martini N: Radiologically occult *in situ* and incipient invasive epidermoid lung cancer: Detection by sputum cytology in a survey of asymptomatic cigarette smokers. Am J Surg Pathol 1:5–16, 1977
5. Trump BF, McDowell EM, Glavin F, Barrett LA, Becci PJ, Schürch W, Kaiser HE, Harris CC: The respiratory epithelium: III. Histogenesis of epidermoid metaplasia and carcinoma in situ in the human. J Natl Cancer Inst 61:563–575, 1978
6. Nettesheim P, Griesemer R: Experimental models for studies of respiratory tract carcinogenesis, Pathogenesis and Therapy of Lung Cancer. Edited by CC Harris. New York, Marcel Dekker, 1978, pp 75–188
7. Klein-Szanto AJP, Topping DC, Heckman CA, Nettesheim P: Ultrastructural characteristics of carcinogen-induced dysplastic epithelial changes in tracheal epithelium. Am J Pathol (In press)
8. Klein-Szanto AJP, Olson AC, Nettesheim P: Quantitative study of carcinogen-induced epithelial lesions in tracheal epithelium (In preparation)
9. Topping D, Nettesheim P: Quantitative assessment of sequential epithelial changes in tracheal mucosa following exposure to DMBA. Cancer Res (In press)
10. Topping D, Nettesheim P: Development and fate of focal lesions in tracheal mucosa following carcinogen exposure. Cancer Res (In press)
11. Topping DC, Pal BC, Martin DH, Nelson FR, Nettesheim P: Pathological changes induced in respiratory tract mucosa by polycyclic hydrocarbons of differing carcinogenic activity. Am J Pathol 93:311–324, 1978
12. Mowry RW, Winkler CH: The coloration of acidic carbohydrates of bacteria and fungi in tissue sections with special reference to capsules of *Cryptococcus neoformans*, pneumococci and staphylococci. Am J Pathol 32:628–629, 1956
13. Dirksen ER, Crocker TT: Ultrastructural alterations produced by polycyclic aro-

matic hydrocarbons on rat tracheal epithelium in organ culture. Cancer Res 28:906–923, 1968
14. Dahlgren SE, Dalen H, Dalhamn T: Ultrastructural observations on chemically induced inflammation in guinea pig trachea. Virchows Archiv (Cell Pathol) 11:211–223, 1972
15. Asmundsson T, Kilburn KH, McKenzie WN: Injury and metaplasia of airway cells due to SO_2. Lab Invest 29:41–53, 1973
16. Gordon RE, Lane BP: Regeneration of rat tracheal epithelium after mechanical injury: II. Restoration of surface integrity during the early hours after injury. Am Rev Respir Dis 113:799–807, 1976
17. Philpott DE, Harrison GA, Turnbill C, Black S: Ultrastructural changes in tracheal epithelial cells exposed to oxygen. Aviat Space Environ Med 48:812–818, 1977
18. Becci PJ, McDowell EM, Trump BF: The respiratory epithelium: IV. Histogenesis of epidermoid metaplasia and carcinoma in situ in the hamster. J Natl Cancer Inst 61:577–586, 1978
19. Klein-Szanto AJP: Clear and dark basal keratinocytes in human epidermis. J Cutan Pathol 4:275–280, 1977
20. Raick AN: Ultrastructural, histological, and biochemical alterations produced by 12-*O*-tetradecanoyl-phorbol-13-accetate on mouse epidermis and their relevance to skin tumor promotion. Cancer Res 33:269–286, 1973
21. Lupulescu A, Pinkus H: Electron microscopic observations on rat epidermis during experimental carcinogenesis. Oncology 33:24–28, 1976
22. Frithiof L: Ultrastructure of the basement membrane in normal and hyperplastic human oral epithelium compared with that in preinvasive and invasive carcinoma. Acta Pathol Microbiol Scand 200 (Suppl):1–63, 1969
23. Smith CJ: The epithelial-connective tissue junction in the pathogenesis of human and experimental oral cancer, Tissue Interactions in Carcinogenesis. Edited by D Tarin. London, Academic Press, 1972, pp 191–225
24. Takarada H, Cattoni M, Sugimoto A, Rose GG: Ultrastructural studies of human gingiva: III. Changes of the basal lamina in chronic periodontitis. J Periodontol 45:288–302, 1974
25. Kilburn KH, McKenzie WN: Leukocyte recruitment to airways by aldehyde-carbon combinations that mimic cigarette smoke. Lab Invest 38:134–142, 1978
26. Barrett LA, McDowell EM, Harris CC, Trump BF: Studies on the pathogenesis of ischemic cell injury: XV. Reversal of ischemic cell injury in hamster trachea and human bronchus by explant culture. Beitr Pathol 161:109–121, 1977

Acknowledgments

We appreciate the expert technical assistance of Mrs. Alice Pine and Mr. Don Martin and gratefully acknowledge the generous cooperation of Dr. D. C. Swarztendruber, Oak Ridge Associated Universities, who permitted the use of his electron microscope facilities.

[*Illustrations follow*]

Figure 1—Hypotrophic epithelium of cuboidal type showing PAS-positive material in the cytoplasm (*arrows*); 200 μg DMBA, 24 weeks. (PAS, ×360)

Figure 2—Hypotrophic epithelium of squamous (simple) type; 200 μg DMBA, 48 weeks. (Toluidine blue, ×360)

Figure 3—Hypotrophic epithelium. Cuboidal cell with very well developed Golgi complex, in association with large amounts of secretory vesicles (*arrows*), rough endoplasmic reticulum, lamellated body, and an "intracytoplasmic" microcyst (*asterisk*); 200 μg DMBA, 24 weeks. (×7700)

Figure 4—Nonkeratinizing squamous metaplasia; large cells with prominent nuclei and nucleoli and a superficial microcyst (*arrow*); 200 μg DMBA, 12 weeks. (Toluidine blue, ×360)

Figure 5—Keratinizing squamous metaplasia of the acanthotic type exhibiting orthokeratinization and numerous darkly staining cylindrical basal epithelial cells; 200 μg DMBA, 48 weeks. (Toluidine blue, ×360)

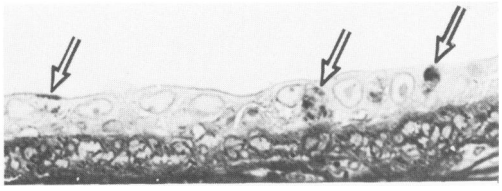

1

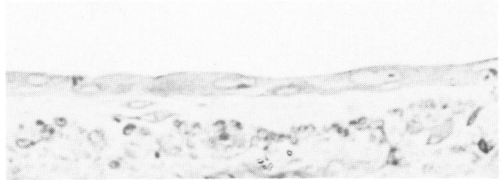

2

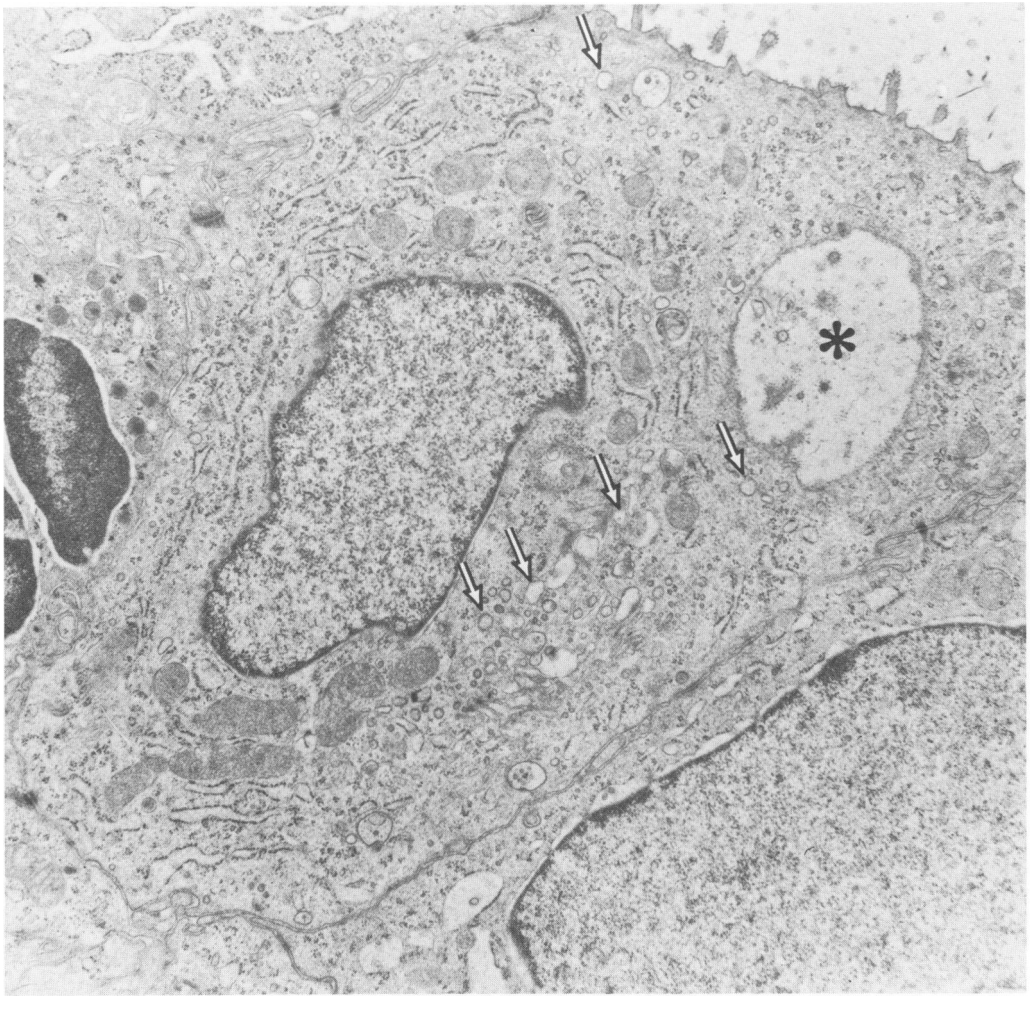

3

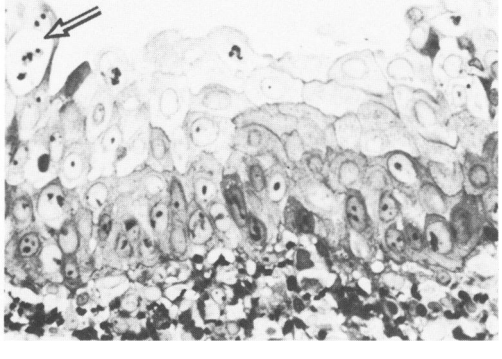

4

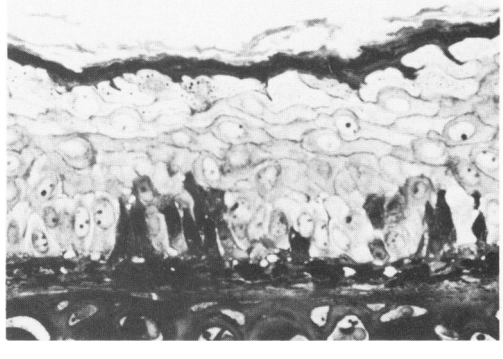

5

Figure 6—Nonkeratinizing squamous metaplasia. Superficial "umbrella" cell straddling several cells. Note large number of microgranules in the apical portion of cells; 200 μg DMBA, 12 weeks. (×4200)

Figure 7—Nonkeratinizing squamous metaplasia. Superficial cell exhibits organelles, tonafilament bundles (*TB*), and numerous cytoplasmic droplets (*CD*) compatible with mucin secretion. Nonepithelial cell (*NE*); 200 μg DMBA, 24 weeks. (×6000)

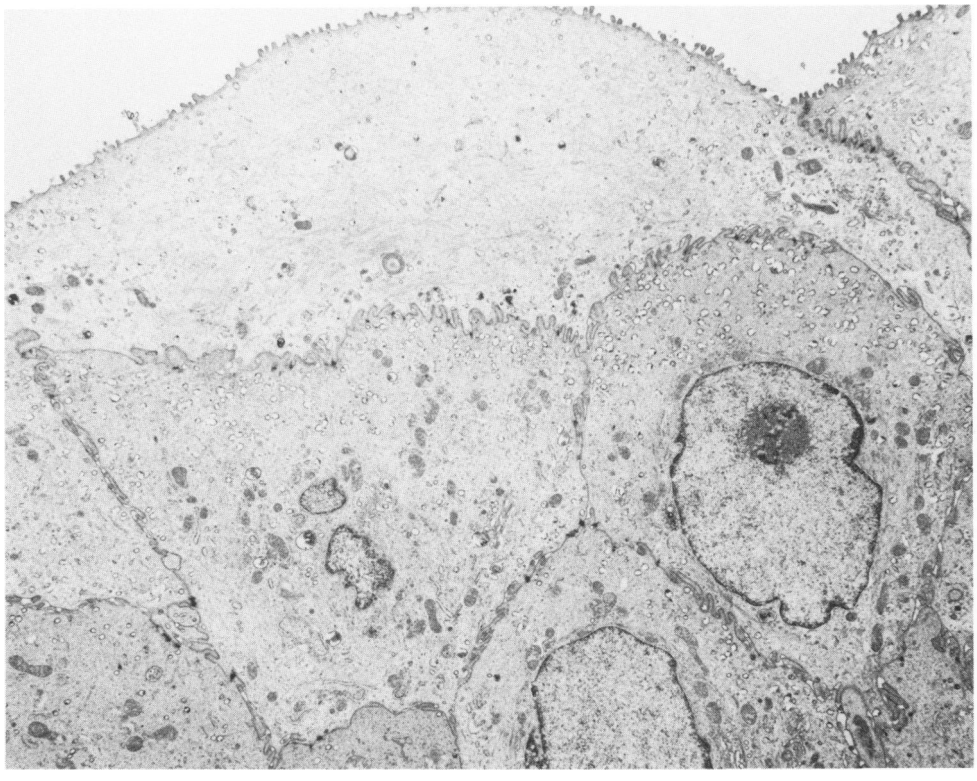

6

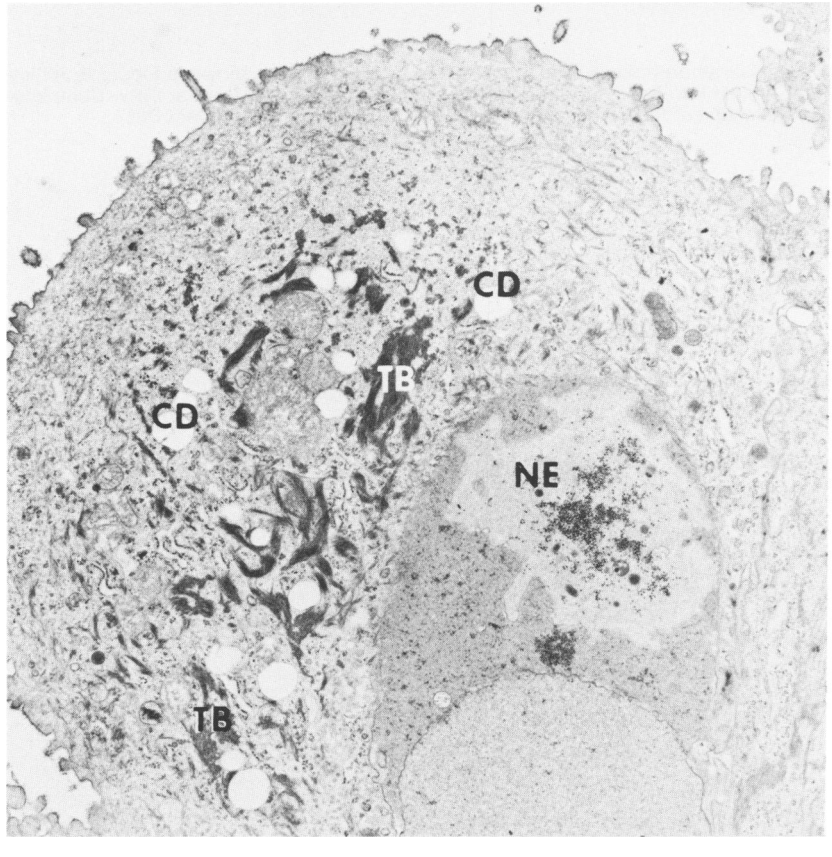

7

Figure 8—Keratinizing squamous metaplasia of the atrophic type; 200 μg DMBA, 48 weeks. (Toluidine blue, ×360)

Figure 9—Ultramorphologic characteristics of the same lesion shown in Figure 8. All layers present typical keratinocyte features with no indication of secretory activity. Complete orthokeratinization of the horny layer (*HL*). Basal lamina (*bl*), basal layer (*BL*).

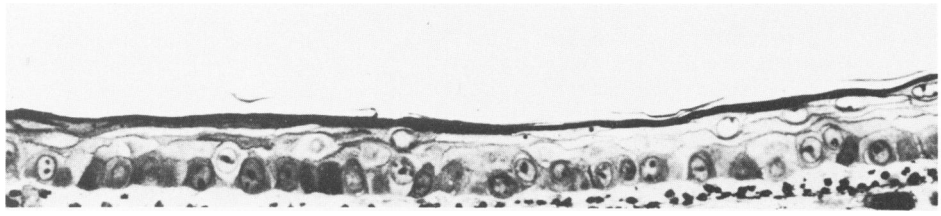

8

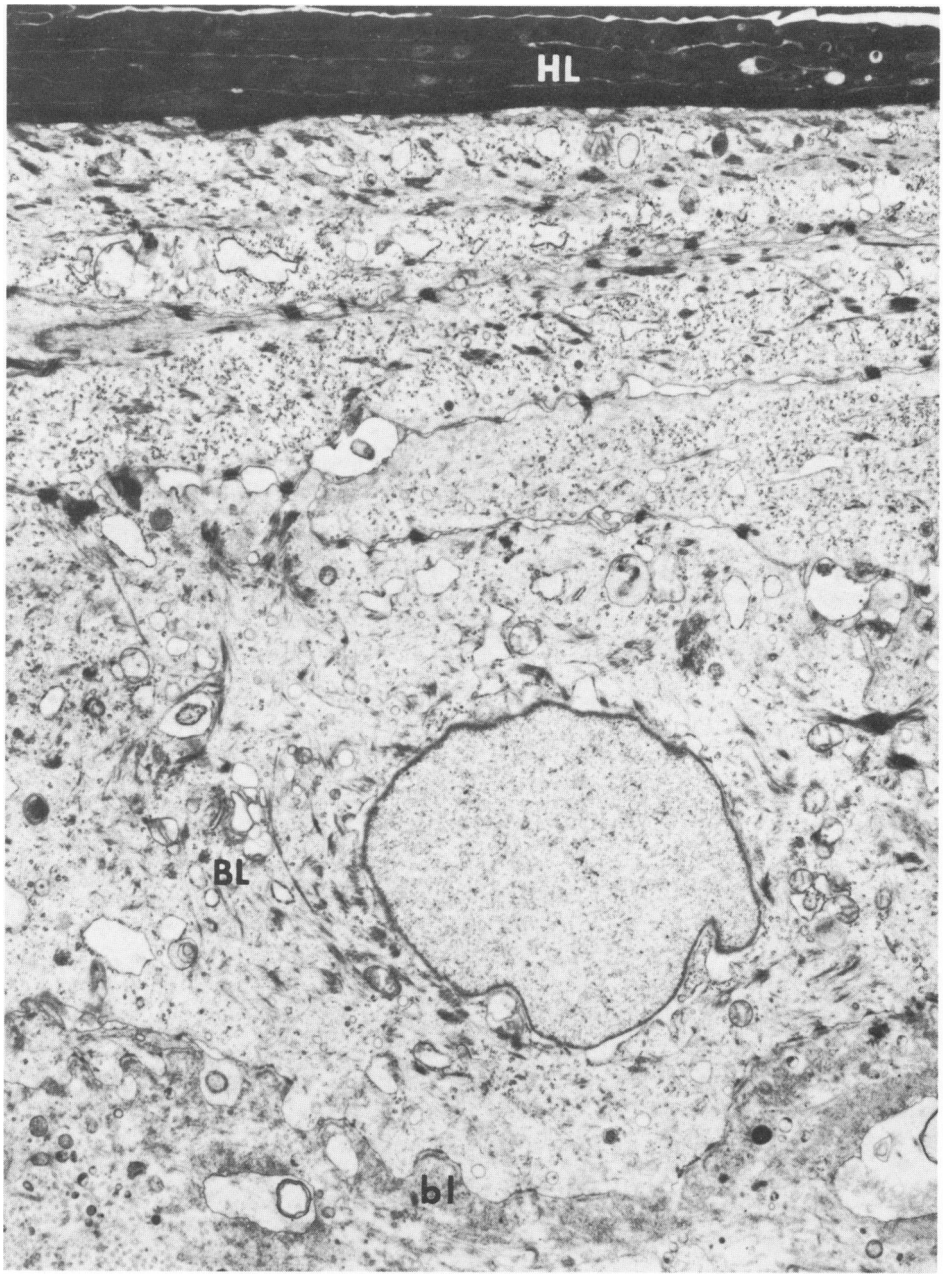

9

Figure 10—Keratinizing squamous metaplasia. Dark epithelial basal cells usually of fusiform shape, rich in ribosomes, mitochondria, and densely packed cytoplasmic filaments and having an electron-dense nucleus; 200 μg DMBA, 24 weeks. (×7300)

Figure 11—Keratinizing squamous metaplasia. Clear epithelial basal cell, more ovoid in shape, and showing similar but much less compactly arranged components than the dark cell in Figure 10. In addition, this cell exhibits more ergastoplasm, Golgi complexes, and lysosomes; 200 μg DMBA, 24 weeks. (×7300)

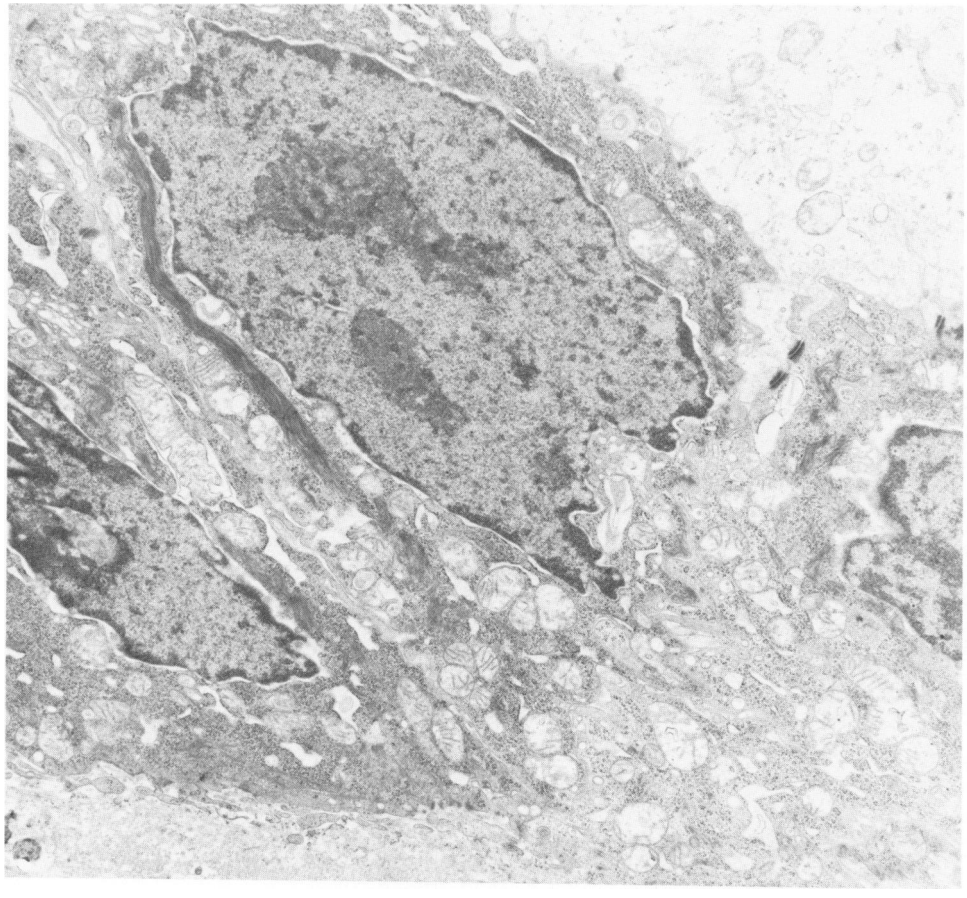

10

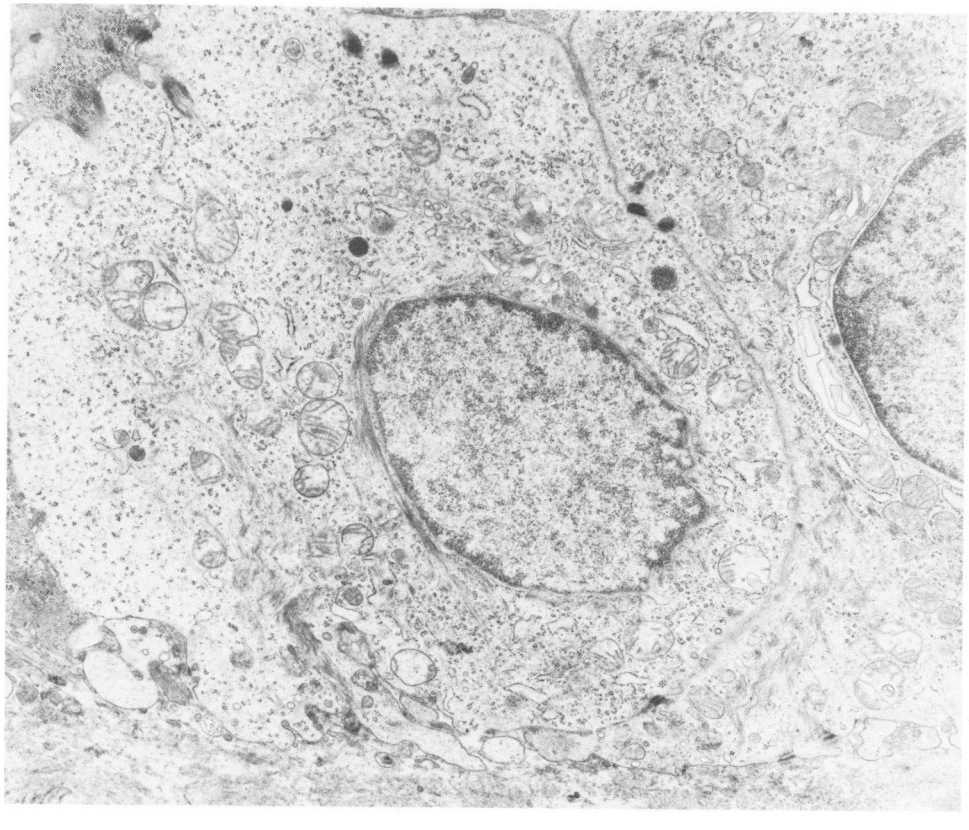

11

Figure 12—Keratinizing squamous metaplasia. Basal cells (*BC*) in direct contact with the connective tissue (*arrows*). The basal lamina is not visible. Collagen fibers (*c*). (×11,000)

Figure 13—Nonkeratinizing squamous metaplasia. Epithelial cell of the spinous layer showing intense perinuclear centralization of tonofilament bundles (*arrows*). Note filament-free exoplasm; 200 μg DMBA, 24 weeks. (×5000)

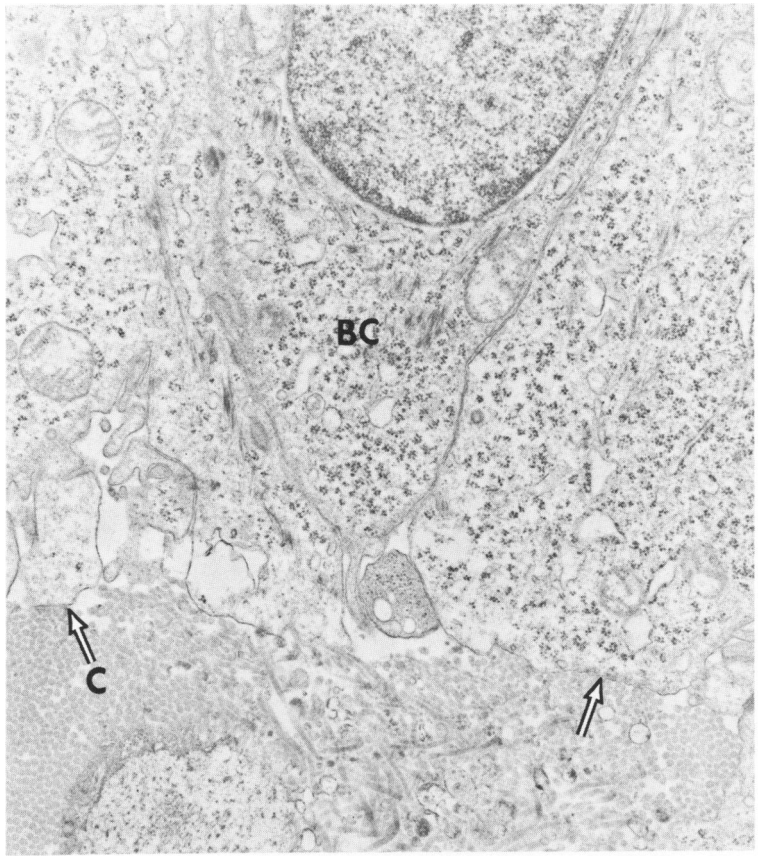

12

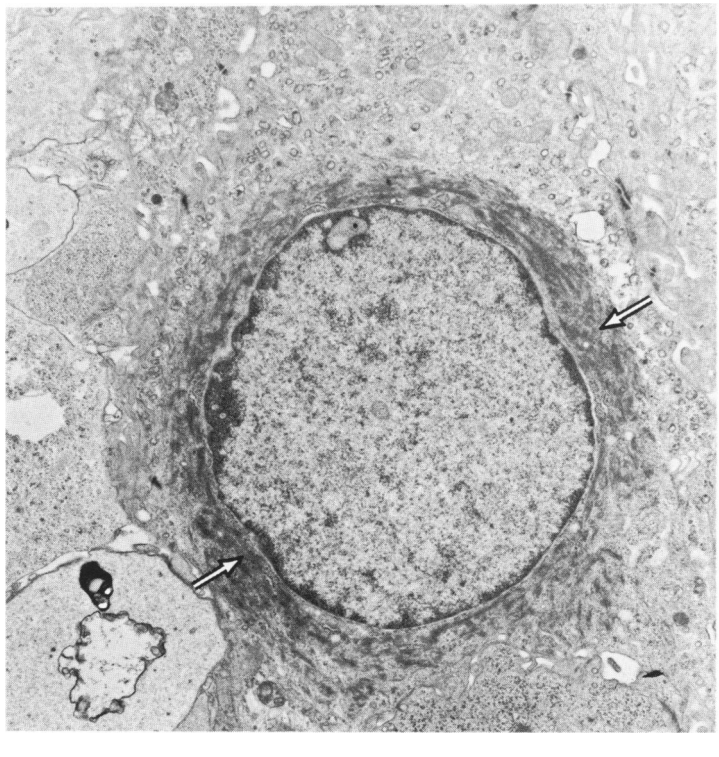

13

Figure 14—Early nonkeratinizing squamous metaplasia. Superficial half of the epithelium exhibiting positive AB staining indicative of the presence of acid mucosubstances; 200 μg DMBA, 2 weeks. (PAS–AB, pH 2.6, ×360)

Figure 15—Early nonkeratinizing squamous metaplasia characterized by large spinous cells with hypertrophic nuclei and nucleoli, and several nonepithelial inflammatory cells (*NE*); 200 μg DMBA, 2 weeks. (×2400)

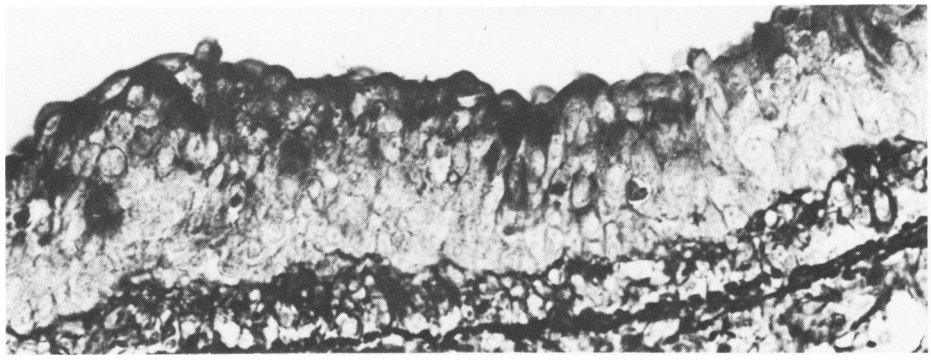

14

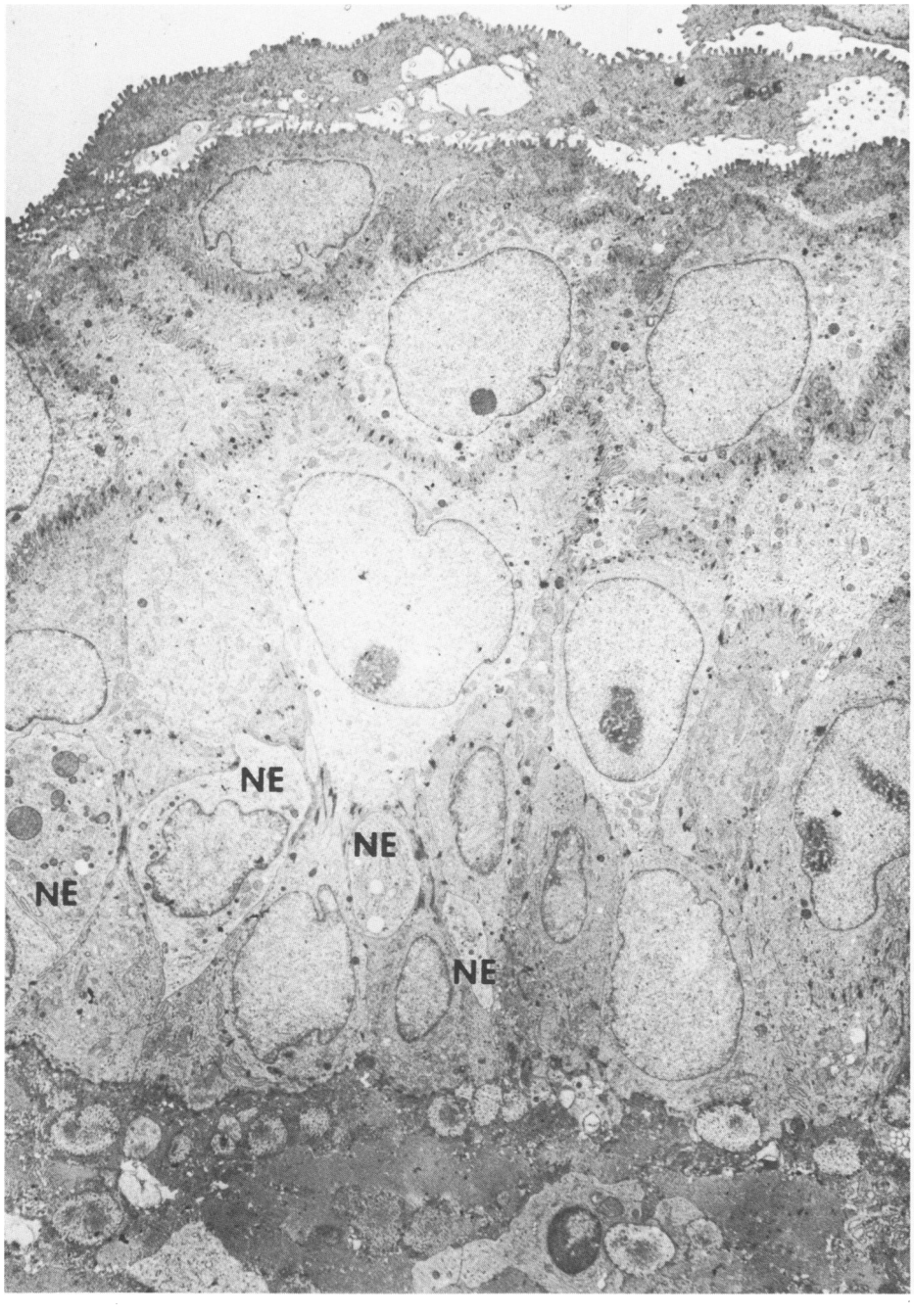

15

[*End of Article*]